







# Development of coal-derived carbon-based structural unit as a potential new building material

Md Tarik Hossain<sup>1</sup> , Chooikim Lau<sup>2</sup> , Hua Yu<sup>1</sup> , and Kam Ng<sup>1,\*</sup> 

<sup>1</sup>Department of Civil and Architectural Engineering and Construction Management, University of Wyoming, 1000 E. University Avenue, Laramie, WY 82071, USA

<sup>2</sup>Center for Carbon Capture and Conversion, School of Energy Resources, University of Wyoming, 1000 E. University Avenue, Laramie, WY 82071, USA

**Received:** 17 September 2022

**Accepted:** 26 December 2022

**Published online:**

2 January 2023

© The Author(s), under exclusive licence to Springer Science+Business Media, LLC, part of Springer Nature 2023

## ABSTRACT

Coal combustion for energy has not only wasted the hydrogen-rich volatile matters but also results in CO<sub>2</sub> emission causing serious environmental issues. An integrated coal pyrolysis and solvent extraction process under elevated temperatures in an inert atmosphere is implemented to convert as-mined coal from Wyoming Powder River Basin to functional carbon elements such as pyrolysis char (PC). This paper presents the development and fabrication of new carbon-based structural unit (CSU) using pulverized PC and two coal-derived pitches (mesophase pitch and tar pitch) to attain high compressive strength greater than 30 MPa, low thermal conductivity less than 0.30 W/m K, and low density less than 1.25 g/cm<sup>3</sup>. CSUs have the potential to overcome the current challenges with cement and concrete through pressurized fabrication followed by carbonization. This study aims to develop CSU with nearly 100% coal-derived carbon material for structural application in buildings. The effects of pressing pressures, carbonization temperatures, and binder contents on the density and mechanical and thermal properties of CSU samples are investigated. The study concludes that mesophase pitch produces a better performance of CSU samples, a combination of 100 MPa pressing pressure and carbonization temperature of 900 °C yields the highest compressive strength, and a 25% MP content is recommended for low-cost CSU fabrication. CSU has a much lower density, lower thermal conductivity, higher compressive strength, and higher strength-to-density ratio than normal concrete.

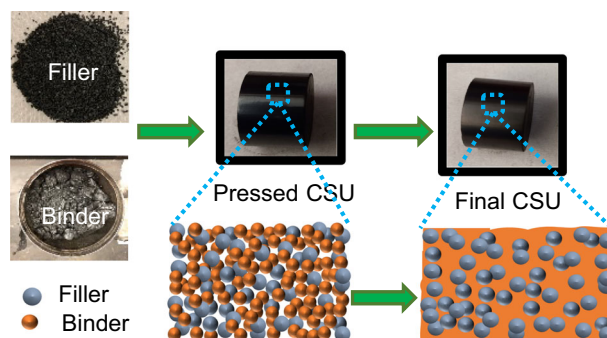
Handling Editor: Maude Jimenez.

Address correspondence to E-mail: kng1@uwo.edu

E-mail Addresses: mhossai2@uwo.edu; clau1@uwo.edu; hyu3@uwo.edu

<https://doi.org/10.1007/s10853-022-08129-0>

## GRAPHICAL ABSTRACT

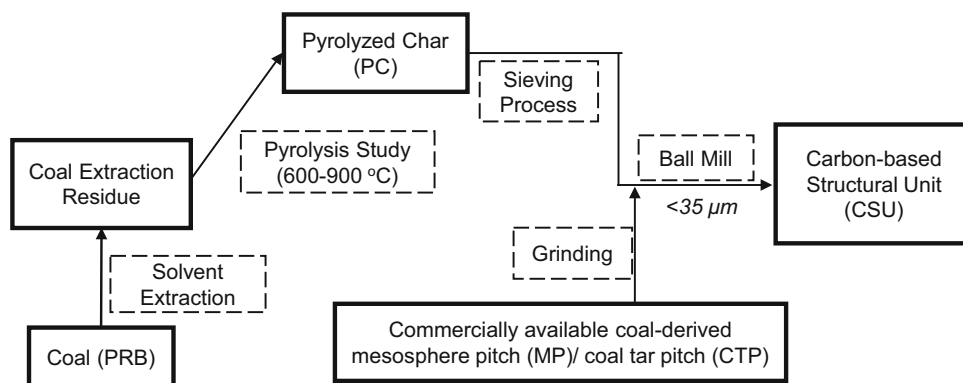


## Introduction

Coal is a limited and non-renewable carbonaceous fossil fuel containing mostly carbon with variable amounts of other elements, chiefly hydrogen, sulfur, oxygen, and nitrogen [1]. Coal, as a carbon-rich resource, is considered the “dirtiest” of fossil fuels in terms of carbon dioxide production from direct coal combustion. Direct combustion of coal for energy supply not only wastes hydrogen-rich volatile matter but also results in serious pollution. Therefore, the alternative conversion of coals into carbon-based materials for building construction instead of direct combustion has attracted increasing attention [2, 3]. Coal can be pyrolyzed to produce volatile and pyrolyzed char (PC), followed by the separation of volatile for pyrolyzed gas and tar Zhang et al. [4]. An integrated coal pyrolysis and solvent extraction process under elevated temperatures in an inert atmosphere has been invented at the University of

Wyoming (UW) under the patent (WO 2019/0055529) to convert as-mined coal to functional carbon elements, such as PC. Figure 1 illustrates the technical process of manufacturing the PC as well as other extracts and residues from the Wyoming Powder River Basin (PRB) coal. Comprehensive use of coal and coal-derived materials has been extensively investigated for a wide range of innovative applications such as activated carbon [5–7], carbon fiber [8–10], carbon foam [11–13], graphene/carbon dots [14–16], ceramics [17, 18], and construction materials [2, 19]. The PC, obtained at low temperatures, has different applications, such as combustion for heat [20, 21], gasification of char solids for organics, and soil amendment [22, 23]. A large proportion of fixed carbon will be retained in solid residue after the gasification process. The conventional approaches of utilizing PCs would not be environmentally friendly or cost-effectively. For example, direct combustion of PC will release carbon dioxide and other air pollutants, resulting in severe environmental issues [2].

**Figure 1** Coal pyrolysis and solvent extraction process to convert coal as PC for CSU fabrication.



However, a promising application is to utilize the PC as a building material for structural elements like a beam, column, and foundation. Very limited studies [3, 24] have been conducted to use coal-char to produce carbon-based construction materials that are comparable to building materials, such as normal concrete and concrete masonry. These researchers fabricated disks of 12 mm diameter by 6 mm thick from pulverized metallurgical coke bonded with coal tar pitch (CTP), followed by carbonization. They reported tensile strengths ranging from 10 to 60 MPa and densities ranging from 1.01 to 1.24 g/cm<sup>3</sup> depending on the composition which is stronger and lighter than normal concrete. In the previous studies, only split tensile strength and densities have been investigated for disk samples prepared with coke and CTP and compared with OPC. But it is more important to investigate compressive strength, which is emphasized in this research, along with the other properties of the carbon building materials to compare with concrete as concrete is used mostly to resist compression.

Carbon-based building materials can be fabricated from PC and coal-derived mesophase pitch (MP) or coal tar pitch. PC is a solid filler material, and coal-derived MP or CTP works as the binder material. Because of the unique properties of PC, such as considerable specific surface area ( $\sim 275 \text{ m}^2/\text{g}$ ) and porous channel of PC [2], coal-derived MP or CTP can flow into the PC bed and bond with PC during the carbonization process. In addition, coal-derived MP or CTP can be carbonized to form carbon-based building material. The carbon-based material should provide better insulation properties than concrete with relatively lower thermal conductivity due to low density as well as better mechanical strength from carbonization. In addition, concrete has durability problems due to bleeding [25], honeycombing [26], alkali-silica reaction [27], steel corrosion [28], efflorescence [29], and heterogeneity of the materials [30] that cause real challenges for concrete constructions. Concrete is also a major CO<sub>2</sub> emitter causing global warming because it uses cement as a binder and for every ton of cement production almost a ton of CO<sub>2</sub> is emitted [31]. The higher density of concrete added higher dead loads on the structural elements that demand larger cross sections. Carbon-based structural units (CSU) have the potential to overcome the current challenges with concrete constructions through pressurized fabrication followed by

carbonization. In addition, at the end of its serving life, the carbon-based building material could be recycled for soil amendment rather than landfilling. In this way, the environmental issues caused by carbon dioxide emissions could be eliminated through the deposition of carbons in buildings.

In this study, CSUs are developed using pulverized PC and coal-derived mesophase pitch to attain high compressive strength, low thermal conductivity, and low density. The PC powder and pulverized mesophase pitch are mixed by a ball mill and then made into a cylindrical shape with a pressing steel mold followed by carbonization. Regarding serving as a building material, purity is not important for ambient temperature construction, and graphitization is not required. Therefore, the carbonization process can be carried out at relatively low temperatures [3]. This study aims to develop CSU with nearly 100% coal-derived carbon material for structural application in buildings such as load-bearing structural elements. The CSU should have high mechanical strength (compressive strength > 30 MPa), lightweight (density < 1.25 g/cm<sup>3</sup>), and high thermal-insulating property (thermal conductivity < 0.30 W/m.K).

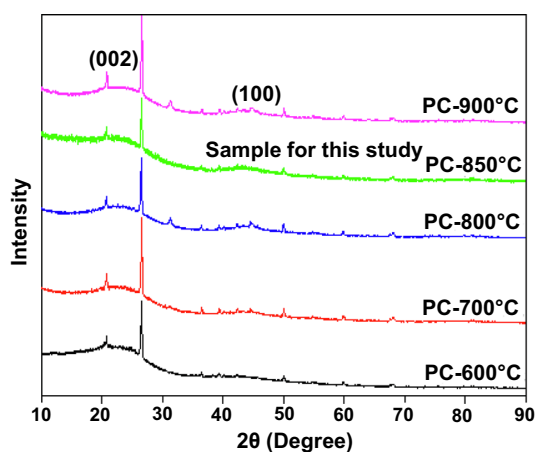
## Materials and methods

### Pyrolyzed char

The PCs produced from the Wyoming PRB coal are obtained after pyrolyzed at a temperature of 850 °C, and the yield rate of PCs from coals is 46.3%. The chemical composition of the PC is given in Table 1 where the major components are determined by proximate analysis and the metal contents are determined by X-ray fluorescence (XRF). It shows the dominant material is fixed carbon while a small amount of few metals (chromium, copper, and lead) are detected. Maximum values for surface coatings and substrates—other than modeling clay—included as a part of a toy are recommended for arsenic < 25 ppm, cadmium < 75 ppm, chromium < 60 ppm, lead < 90 ppm, mercury < 60 ppm, and selenium < 500 ppm [32]. In addition, heavy metal contents in electrical and electronic equipment are regulated to restrict lead < 0.1 wt%, mercury < 0.1 wt%, hexavalent chromium < 0.1 wt%, and cadmium < 0.01 wt% [33]. Accordingly, the PCs from Wyoming PRB coals present extremely low metal

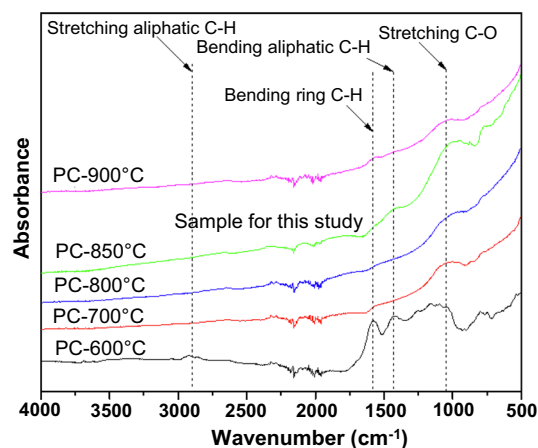
**Table 1** Chemical composition of the pyrolyzed char

Category	Material	Content
Major components	Ash (%)	15.96
	Volatile Matter (%)	1.2
	Fixed Carbon (%)	79.87
	Moisture (%)	2.97
Metal components	Arsenic (mg/kg)	3
	Cadmium (mg/kg)	Not detected
	Chromium (mg/kg)	9
	Copper (mg/kg)	14
	Lead (mg/kg)	1
	Mercury (mg/kg)	Not detected
	Selenium (mg/kg)	Not detected

**Figure 2** XRD patterns of the char samples pyrolyzed at five different temperatures.

contents and meet the requirements of heavy metal content limits specified in the ASTM F963-17 and EU RoHS 2013.

Figure 2 shows the X-ray diffraction (XRD) test results of PC samples pyrolyzed at five temperatures from 600 to 900 °C. The intensive broad peak (0 0 2), which corresponds with the graphitic basal plane, is observed at  $2\theta$  values of 20° to 30°. The broad peak (1 0 0) at about 43° corresponds with the graphitic crystalline features of the PC sample [34]. The slight increase in these peak values with increasing pyrolysis temperature from 600 to 900 °C is attributed to the stable aromatic form of the carbon species. The two sharp peaks are observed at 21–26° and a few moderate peaks are observed at 50°, 60° and 68°, which are attributed to the presence of a low percentage of inorganic silica in all the PC samples.

**Figure 3** FTIR analysis of the char samples pyrolyzed at five different temperatures.

The Fourier transform infrared (FTIR) testing results of the PC samples pyrolyzed at five different temperatures of 600 °C, 700 °C, 800 °C, 850 °C, and 900 °C are compared in Fig. 3. The FTIR results show valuable surface information about the PCs. The decomposition and evaporation of the organic matter during the pyrolysis of coal cause the disappearance of the vibrational bonds and a reduction in the intensity of the bands. The wavenumbers around 2910–1430  $\text{cm}^{-1}$  correspond to the stretching aliphatic CH and bending aliphatic CH, respectively [35]. Although the shapes of the FTIR characteristic curves demonstrate similar peak locations, the weakening and disappearance of the stretching aliphatic and bending aliphatic CH groups for the PC from pyrolysis temperatures of 600–900 °C are attributed to the decomposition of the organic matter, which turns into the graphitic-like carbon. The PC samples obtained from pyrolysis temperatures of 600–900 °C still maintain a significant amount of stretching C–O. The peaks of the stretching C–O bond weaken with the increase in pyrolysis temperature. This could be attributed to the conversion of the C–O bond to possibly carbon monoxide and carbon dioxide escaped during the pyrolysis process involving the decomposition of organic matters at temperatures ranging between 700 and 850 °C. On the other hand, the melting but no decomposition of organic matter at 600 °C yield a slightly different FTIR spectrum and higher stretching C–O bond and other functional groups [2]. A relatively higher stretching C–O bond detected in PC-850 could be attributed to the decomposition of lower organic matter content

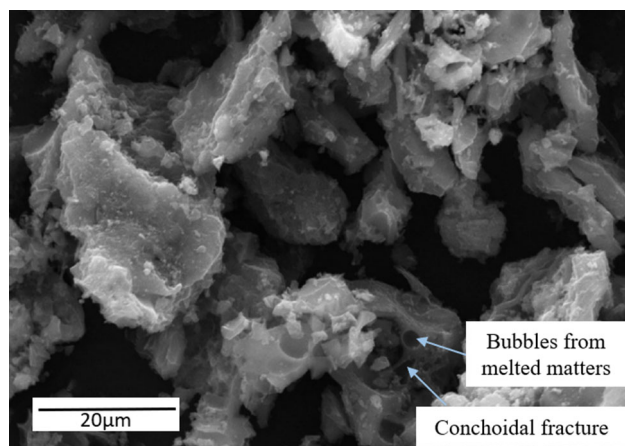


**Figure 4** SEM image of the char sample pyrolyzed at 850 °C.

remained in the PC (only 1.2% volatile matter remained in PC-850 as shown in Table 1) and lesser reactions occurred during the pyrolysis at 850 °C. The increasing degree of graphitization above 900 °C continues to weaken the C–O bond.

This C–O functional group can provide a unique advantage for decomposing unstable hydrocarbons ( $-\text{CH}_x$ ) during oxidation of CSU. The reaction of  $-\text{CH}_x$  and the oxygen-containing groups produces the  $-\text{CH}_2\text{OOH}$ , which further forms the free radicals of  $-\text{CH}_2\text{O}\cdot$  and  $\text{OH}\cdot$ . The  $\text{OH}\cdot$  participates to form the  $\text{H}_2\text{O}$  through hydrogen abstraction, and the  $-\text{CH}_2\text{O}\cdot$  gets stabilized to form hard carbon–carbon bond [36]. Finally, the carbonization process removes heteroatoms from the molecules and forms stable structures in the CSU, which gives rise to excellent mechanical properties.

The scanning electron microscope (SEM) image of the PC pyrolyzed at 850 °C is shown in Fig. 4. The PC presents as a smooth material with conchoidal fractures and rare bubbles that are generated from melted organic matter during the pyrolysis process. These fractures and bubbles leave a cavity in PC and create a considerably high Brunauer–Emmett–Teller (BET) surface area determined from nitrogen porosimetry analysis in accordance with ASTM D6556-21. The BET surface areas of PC are determined as 98  $\text{m}^2/\text{g}$ , 272  $\text{m}^2/\text{g}$ , 270  $\text{m}^2/\text{g}$ , 262  $\text{m}^2/\text{g}$  and 233  $\text{m}^2/\text{g}$  for the corresponding pyrolysis temperatures of 600 °C, 700 °C, 800 °C, 850 °C and 900 °C, respectively [2]. The average pore size of PC is reported as 1.4 nm. High surface area and those cavities increase the contact surface for binding the

MP with PC, which increases the mechanical properties of CSU.

The proximate analysis shows that the volatile matters decrease with the increase in pyrolysis temperature from 20.9% at 600 °C [2] to 1.2% at 850 °C (Table 1). The ultimate analysis shows that the fixed carbon contents increase with the increase in pyrolysis temperature from 69.55% at 600 °C [2] to 79.87% at 850 °C (Table 1). Comparing PC-600, PC-700 and PC-800, PC-850 and PC-900 are better choices as the feedstock for CSU fabrication considering higher fixed carbon, more stable bonds with fewer functional groups, and lower volatile organic matters. On the other hand, PC-850 has a higher BET surface area, a higher sample yield from pyrolysis, and requires lesser energy input than that of PC-900. In addition, the higher C–O functional group in the PC-850 will facilitate the decomposition of unstable hydrocarbons during oxidation stabilization. Thus, PC-850 is selected as the precursor for developing the CSU as a potential building material.

### Mesophase pitch (coal) and coal tar pitch

A commercially available coal-derived mesophase pitch (MP) and a coal tar pitch (CTP) is investigated as a binder in the development of the carbon structural unit (CSU). The softening point is located between 220 and 280 °C for MP and between 140 to 300 °C for CTP. Figure 5 shows the thermogravimetric analysis (TGA) curve of the coal-derived MP sample, and no significant weight loss is observed up to 260 °C. The first relatively large weight loss of about 3% is observed at around 347 °C, which is due to volatilization or decomposition of low molecular weight pitch components. The major weight loss of about 15% is observed at around 650 °C, possibly due to the decomposition of the heavy pitch molecular weight component. Finally, the residual weight at 950 °C is about 66%. Figure 6 shows the TGA curve of the CTP sample, and no significant weight loss is observed up to 120 °C. The first relatively large weight loss of about 2% is observed at around 127 °C, which is due to volatilization or decomposition of low molecular weight pitch components. The major weight loss of about 25% is observed at around 335–435 °C, possibly due to the decomposition of the heavy pitch molecular weight component. Finally, the residual weight at 950 °C is about 50%.

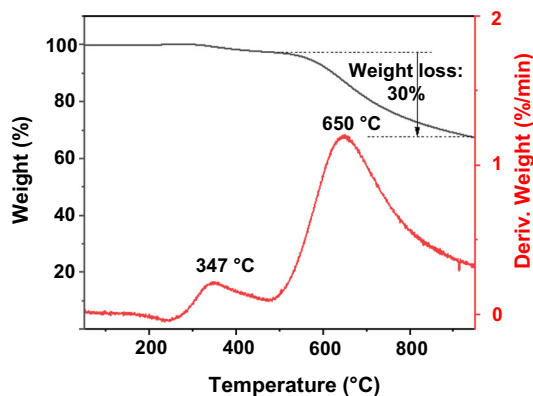


**Figure 5** TGA curve for MP (coal) sample.

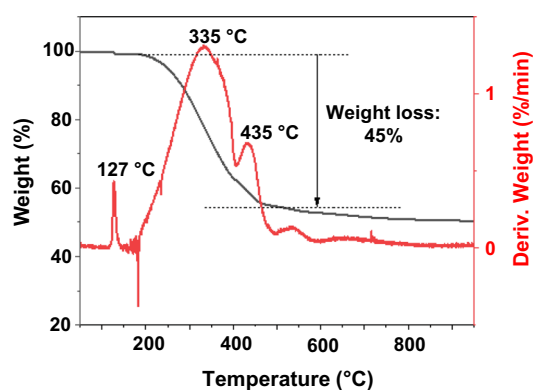


**Figure 6** TGA curve for CTP sample.

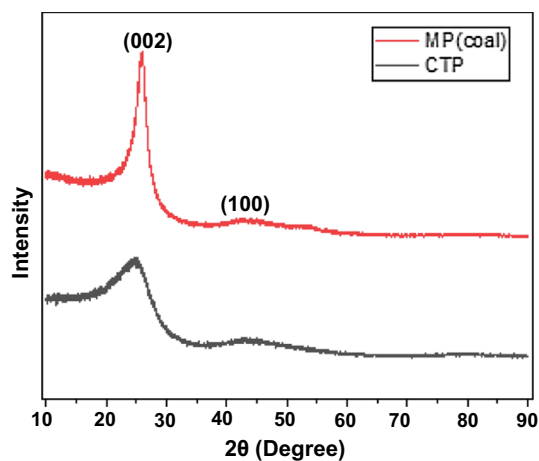


**Figure 7** XRD patterns of MP (coal) and CTP samples.

The XRD spectra of MP and CTP are compared in Fig. 7. The broad diffraction peaks at  $2\theta$  of  $25.4\text{--}43^\circ$  correspond to (002) crystal planes due to the stacking of aromatic layers and (100) crystal face reflection demonstrating the graphitic crystalline feature of the sample, respectively. It is found that the intensity of

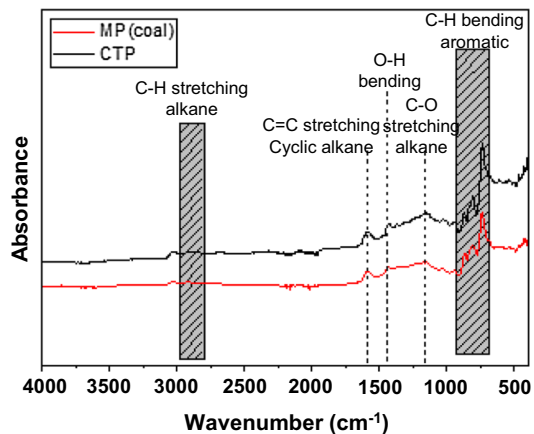


**Figure 8** FTIR spectra of MP and CTP samples.

the peak at  $25.4^\circ$  is higher for MP, indicating a higher stable aromatic form of carbon species in the MP than that in the CTP.

FTIR spectra shown in Fig. 8 indicate valuable information on the surface properties of MP and CTP. The major peaks and corresponding functional groups are indicated in the figure. The peaks around  $3050\text{ cm}^{-1}$  are related to the aromatic C–H stretching. FTIR bands ranging from  $2800\text{ to }3000\text{ cm}^{-1}$  are due to CH stretching alkanes such as aliphatic and alicyclic  $\text{CH}_3$ ,  $\text{CH}_2$ , and CH. The peaks around  $1600\text{ cm}^{-1}$  are from C=C stretching cyclic alkane. Peaks observed in the range of  $700\text{--}900\text{ cm}^{-1}$  are related to aromatic, out-of-plane, and C–H bending [37]. The MP has a slightly higher peak than CTP at  $1200\text{ cm}^{-1}$  for the C–O functional group, which facilitates the decomposition of unstable hydrocarbons [36]. FTIR can be a useful technique to estimate the aromaticity index. The aromaticity indices ( $I_{\text{ar}}$ ) of MP and CTP can be calculated using absorbance values at  $3050\text{ cm}^{-1}$  and  $2920\text{ cm}^{-1}$  given by Eq. (1) [38]. In Eq. (1),  $h_{3050}$  is the peak height of aromatic C–H stretching mode at near  $3050\text{ cm}^{-1}$ , and  $h_{2920}$  is the peak height of aliphatic C–H stretching mode at near  $2920\text{ cm}^{-1}$ . The calculated aromaticity index of MP at 49.97% is slightly higher than 47.91% of the CTP.

$$I_{\text{ar}} = h_{3050} / (h_{3050} + h_{2920}) \quad (1)$$

The shape and shift of the Raman peak of organic materials reveal the atomic and molecular level vibration information of aromatic ring structure [39]. Figure 9 shows the Raman shift of MP and CTP with the major peaks and corresponding functional groups [40]. The MP has higher peak intensity than CTP for

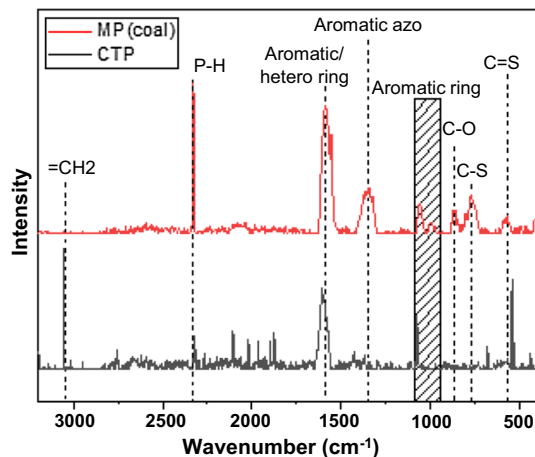


**Figure 9** Raman spectra of MP and CTP samples.

the functional groups of C–S, C–O, aromatic azo and P–H at  $770\text{ cm}^{-1}$ ,  $805\text{ cm}^{-1}$ ,  $1365\text{ cm}^{-1}$ , and  $2330\text{ cm}^{-1}$ , respectively. CTP has higher peak intensity than MP for the functional groups of C=S, alkyne and =CH<sub>2</sub> at  $575\text{ cm}^{-1}$ ,  $2100\text{ cm}^{-1}$ , and  $3050\text{ cm}^{-1}$ , respectively. The higher major aromatic peaks of MP between  $800$  to  $1100\text{ cm}^{-1}$  and at  $1590\text{ cm}^{-1}$  indicate that MP has a higher aromaticity than CTP. This Raman result agrees with that from the FTIR analysis. Hence, MP is expected to be a better binder than CTP in the manufacturing and performance of CSU samples.

### CSU sample fabrication

A new building material known as carbon-based structural units (CSU) is developed by mixing coal-derived MP or CTP with PC from PRB coal in various content ratios, pressing pressures, and carbonization temperatures. In addition, samples made with pure coal-derived MP are also prepared for comparison. Here, the coal-derived MP and CTP work as the binders whereas PC is the solid filler. The procedure for making carbon-based building material samples is illustrated in Fig. 10. The mixture is ball milled in water at 300 rpm for 12 h, dehydrated in an oven at  $150\text{ }^{\circ}\text{C}$  for 24 h, and then compacted into a steel mold to form cylindrical samples under pressing pressure. An oxidation stabilization process is conducted by firstly heating the compacted sample to  $245\text{ }^{\circ}\text{C}$  in an air environment at a rate of  $0.5\text{ }^{\circ}\text{C}/\text{min}$  and holding the sample at this temperature for 12 h before naturally cooling it down to room temperature of  $25\text{ }^{\circ}\text{C}$  at a rate of about  $2\text{ }^{\circ}\text{C}/\text{min}$  to avoid potential thermal

shock in the CSU sample. Next, a carbonization process is conducted by heating the different samples to  $700$ ,  $800$ ,  $900$ ,  $1000$ ,  $1200$ , and  $1600\text{ }^{\circ}\text{C}$ , respectively, under nitrogen flow at a heating rate of  $1\text{ }^{\circ}\text{C}/\text{min}$ . The specific temperature is held for 1 h and cooled down at a cooling rate of  $2\text{ }^{\circ}\text{C}/\text{min}$ . The fabrication of these carbonized cylindrical CSU samples is completed for laboratory testing to determine their properties and performances. A total of 18 batches of CSU samples and at least 3 samples for each batch are fabricated with different binders, mixing ratios, pressing pressures, and carbonization temperatures as presented in Table 2.

### Laboratory tests for CSU samples

FTIR is used to identify the compliment functionality between binder pitch and PC, as well as to compare the chemical functionality of different pitches. The FTIR spectra are recorded on a Nicolet iS50 FTIR spectrometer (Thermo Scientific) using the attenuated total reflectance (ATR) technique. FTIR spectra are obtained by collecting 32 scans at a resolution of  $4\text{ cm}^{-1}$  in the measuring range of  $4000$ – $400\text{ cm}^{-1}$  wavenumbers. XRD is widely used in the determination of the crystallinity of carbonaceous material. XRD is conducted using a Rigaku Smartlab diffractometer with a Cu Ka radiation source, operated at  $40\text{ kV}$  and  $40\text{ mA}$  with an angle of reflection,  $2\theta$ , varied between  $10$  and  $90^{\circ}$ . One carbonized CSU sample from a batch is ground into powder, and this powder is characterized using the FTIR and the XRD tests. Thermal conductivity is measured on each CSU sample using a heat flow meter–Hot Disk TPS 1500 according to ISO 22007–2 [41]. The Hot Disk sensors are designed to be placed between the plane surfaces of two sample pieces of the material to be tested. Power input is maintained at  $200\text{ mW}$  for a measurement time of  $20\text{ s}$ . Hot Disk Thermal Analyzer-7.3 software is used to run the test and calculate the thermal conductivity. Two CSU samples are used for the thermal conductivity test, and each test is run three times by flipping the samples each time to determine the average thermal conductivity. After each test, probing depth is checked against the sample thickness to ensure the heat flow does not reach the outside sample surface. The compressive strength of the carbonized CSU samples is measured using Zwick/Roell Z020 compression testing machine through a force-controlled test. A  $20\text{-kN}$  load cell

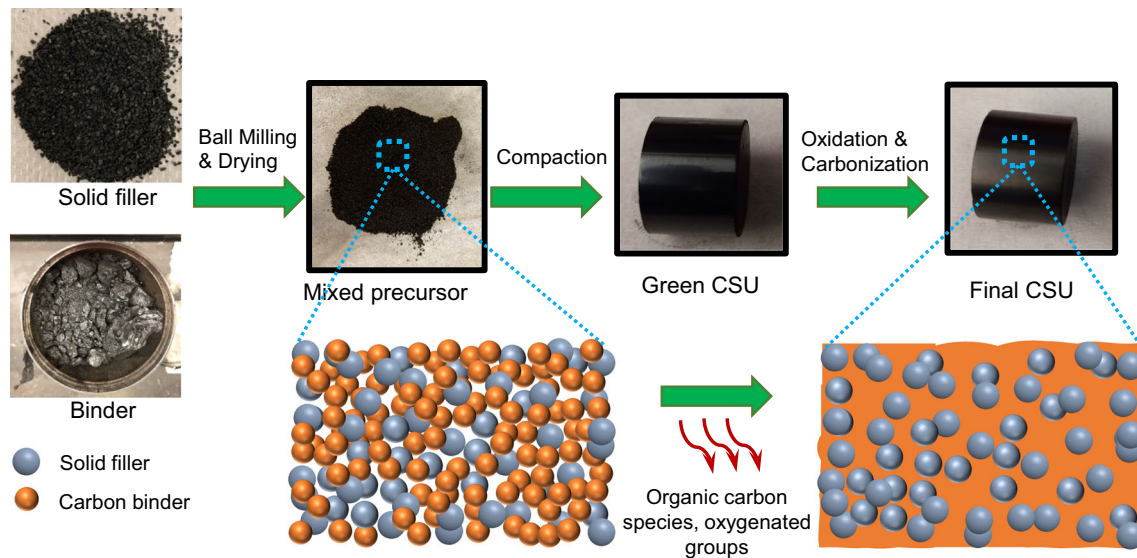


**Figure 10** Fabrication of CSU samples.

**Table 2** CSU samples are fabricated with different parameters

Batch number	Testing parameters	CSU components	Pressing pressure (MPa)	Carbonization temperature (°C)			
1	CTP and MP as a binder	CTP: PC = 1:2	100	1200			
2				1600			
3				1200			
4				1600			
5	Pressing pressure	MP: PC = 1:2	100	700			
6			200				
7			400				
8	Carbonization temperature	MP: PC = 1:2	100	700			
9				800			
10				900			
11				1000			
12				1200			
13				1600			
14				Binder content	MP: PC = 1:4	100	900
15					MP: PC = 1:3		
16					MP: PC = 1:2		
17					MP: PC = 1:1		
18	MP: PC = 1:0						

with an extensometer is used with a loading rate of 200 kPa/s. The cylindrical CSU samples are placed between steel plates, and the axial load is applied until the axial stress passes the peak and reduces with increasing axial strain. A 5-N seating-load with a loading rate of 5 mm/min is applied to the sample to secure the sample position. TestXpert III-V1.2 software is used to operate the testing procedure, collect the stress–strain data, and calculate the maximum

compressive strength. Two to three CSU samples are tested in compression to get the average compressive strength. The types of equipment used at UW for FTIR analysis, XRD patterns, compression test and thermal conductivity test are shown in Fig. 11. The bulk density of the sample is calculated from the measured sample geometry and mass after carbonization.



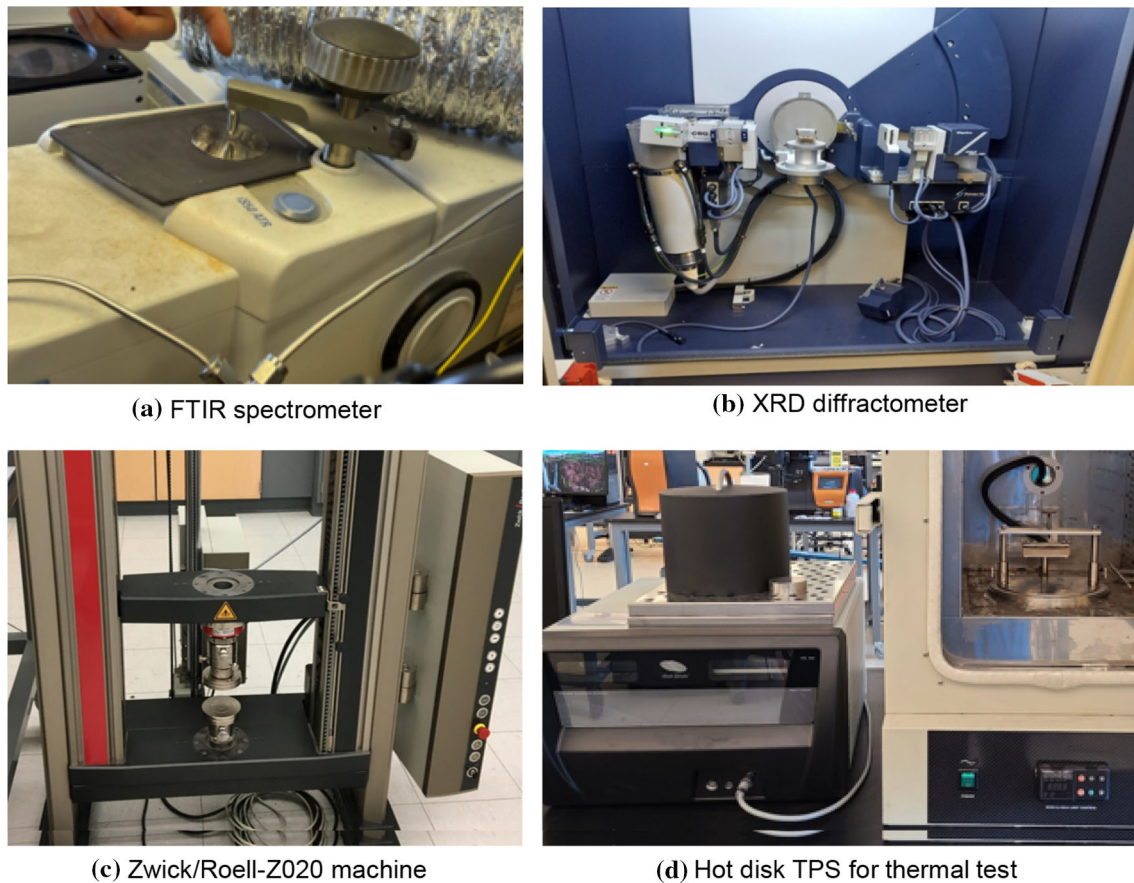


**Figure 11** UW equipment used for **a** FTIR, **b** XRD, **c** compression and **d** thermal tests.

## Results and discussions

### Performances of CTP and MP as binders

The performances of CTP and MP as binders are compared using test results of CSU samples with a mixing ratio of binder (CTP or MP): PC = 1:2. Those samples are prepared with a pressing pressure of 100 MPa and at two different carbonization temperatures of 1200–1600 °C. The density, compressive strength and thermal conductivity comparison are presented in Figs. 12, 13 and 14, respectively. The density of CSU samples after carbonization is close to 1 g/cm<sup>3</sup> for both the samples fabricated with CTP and MP. The density of CSU samples with MP has slightly higher densities than the densities of CSU samples with CTP for both carbonization temperatures. The thermal conductivities of 0.34–0.52 W/m.K are measured for the CSU samples with MP at 1200 °C and 1600 °C, respectively, whereas the CSU samples with CTP have a higher thermal conductivity of 0.46–0.69 W/m.K, at 1200 °C and 1600 °C,

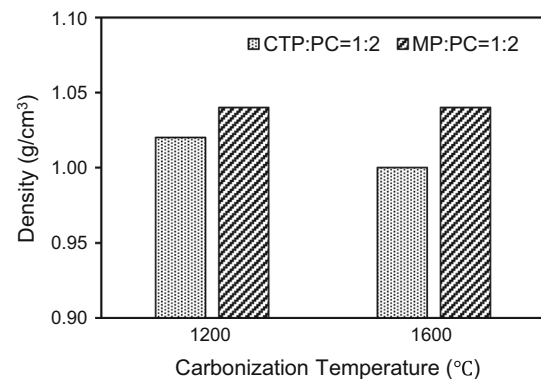


**Figure 12** Density comparison for the CSU samples with CTP and MP.

respectively. The compressive strengths of 61.7 MPa and 47.1 MPa are determined for CSU samples with MP at 1200 °C and 1600 °C, respectively. The decrease in compressive strength of CSU with MP at 1600 °C is most probably due to 1) the higher degree of graphitization that exceeds the optimal degree of graphitization at about 900 °C, and 2) the collapse

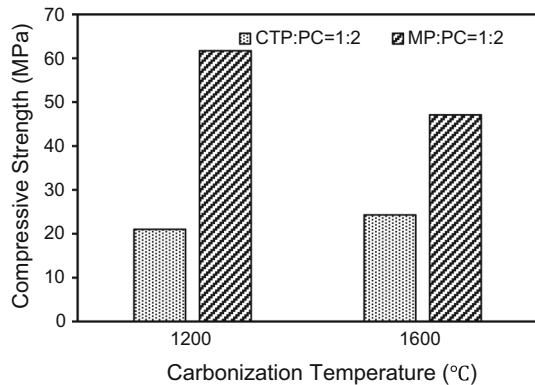


**Figure 13** Compressive strength comparison for the CSU samples with CTP and MP.

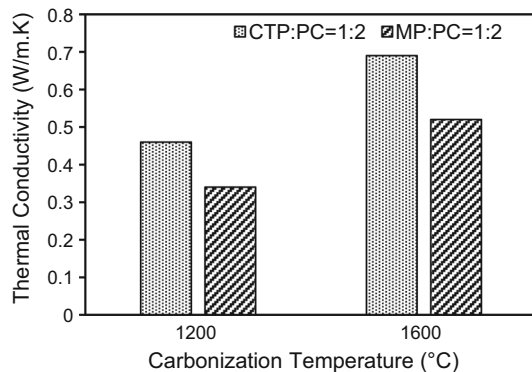


**Figure 14** Thermal conductivity comparison for the CSU samples with CTP and MP.

and/or shrinkage of carbon structure under such high temperature. The optimal degree of graphitization is referenced to the maximum compressive strength of the CSU samples carbonized at 900 °C (Fig. 19).

On the other hand, the CSU samples with CTP have lower compressive strengths of 21–24.3 MPa at 1200 °C and 1600 °C, respectively. The slight increase in compressive strength at 1600 °C could be attributed to a lower degree of graphitization than that experienced in MP, a much higher optimal degree of graphitization, and the continuous decomposition of organic matters. The different degrees of graphitization between MP and CTP at temperatures greater than 900 °C can be differentiated using the TGA results shown in Fig. 5 indicating faster weight loss (or higher degree of graphitization) in MP and in Fig. 6 indicating slower weight loss (or lower degree of graphitization) in CTP. This suggests that the optimal degree of graphitization in the CTP occurs at a higher temperature possibly greater than 1600 °C.

The higher compressive strength of CSU samples fabricated with MP at both carbonization temperatures is attributed to 1) the higher peak for the C–O functional group, which facilitates the decomposition of unstable hydrocarbons and induces stronger carbon–carbon bonds [36], and 2) a higher aromatic index that indicates a stronger carbon–carbon bond matrix. These characteristics are confirmed by both FTIR and Raman spectra as discussed in Sect. “Mesophase pitch (coal) and coal tar pitch”. Considering the higher compressive strength and lower thermal conductivity, MP works better as a binder than CTP in the development of CSU samples. Hence, a comprehensive study is conducted on CSU samples with MP to optimize the properties based on different pressing pressures, carbonization temperatures, and percent MP contents.

### Effect of pressing pressures

To investigate the effect of pressing pressure, CSU samples are fabricated at an MP to PC mass ratio of 1:2 with three different pressing pressures of 100 MPa, 200 MPa and 400 MPa, and then carbonized at 700 °C. The density, compressive strength and thermal conductivity comparison are presented in Figs. 15, 16, and 17, respectively. The density of the carbonized CSU samples increases from 0.97 g/cm<sup>3</sup> at 100 MPa to 1.09 g/cm<sup>3</sup> or 12% at 200 MPa and 1.53 g/cm<sup>3</sup> or 40% at 400 MPa. Increasing the pressing pressure from 100 to 200 MPa significantly increases the compressive strength from 42.7 to 85.6 MPa or by about 100%. With the increase in pressing pressure, the CSU samples are more compacted, the particles are packed closer together, and the voids between the particles reduce. All these factors contribute to the increase in the compressive strength. However, the increase in the pressing pressure does not necessarily yield the same improvement in thermal conductivity. In fact, the thermal conductivity increases slightly from 0.175 to 0.185 W/m.K with the increase in pressing pressures from 100 to 200 MPa. Further increasing the pressing pressure to 400 MPa only increases the compressive strength from 85.6 to 91.5 MPa (i.e., 6.4% improvement) and does not result in the same 100% increases in mechanical properties as observed from 100 to 200 MPa. In addition, the thermal conductivity increases from 0.185 to 0.282 W/m.K or 52.4% when the pressing pressure increases from 200 to 400 MPa.

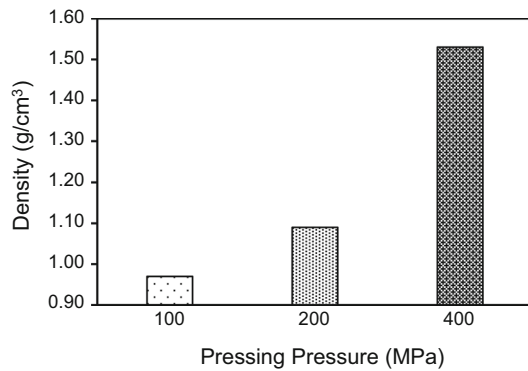


**Figure 15** Effect of pressing pressures on the density of CSU carbonized at 700 °C.

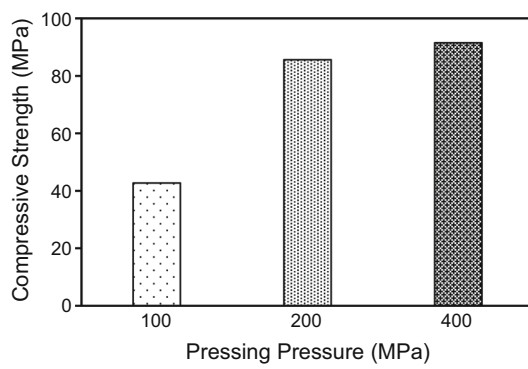


**Figure 16** Effect of pressing pressures on compressive strength of CSU carbonized at 700 °C.

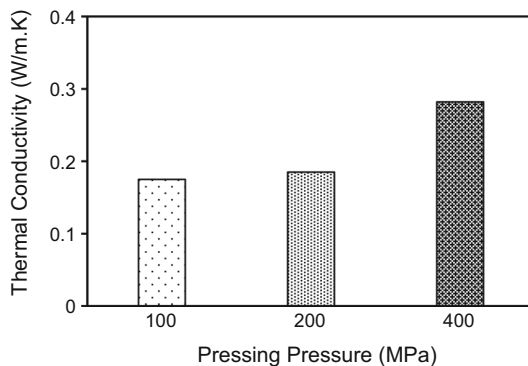


**Figure 17** Effect of pressing pressures on thermal conductivity of CSU carbonized at 700 °C.

Therefore, to attain a relatively high compressive strength and low thermal conductivity, the pressing pressures of 100–200 MPa are further investigated to determine the optimum carbonization temperature.

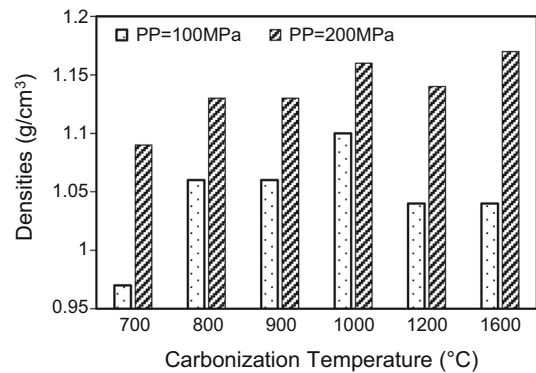


**Figure 18** Densities of CSU samples (MP: PC = 1:2) at six different carbonization temperatures.

### Effect of carbonization temperatures

To understand the effects of carbonization temperatures on the mechanical and thermal properties of CSU samples, a more comprehensive study is carried out considering two pressing pressures (100–200 MPa) and six carbonization temperatures (700 °C, 800 °C, 900 °C, 1000 °C, 1200 °C, and 1600 °C). The density comparison for the two pressures at different carbonization temperatures is shown in Fig. 18. For the pressing pressure of 100 MPa, the density of the carbonized CSU samples increases from 0.97 g/cm<sup>3</sup> at 700 °C, 1.06 g/cm<sup>3</sup> at both 800 °C and 900 °C and to the highest of 1.10 g/cm<sup>3</sup> at 1000 °C due to the carbonization. The density reduces to 1.04 g/cm<sup>3</sup> at both 1200 °C and 1600 °C due to the combination of continuous weight loss, expansion of pore volume, reappearance of pores, and the collapse of carbon structure. For the pressing pressure of 200 MPa, the density increases from 1.09 g/cm<sup>3</sup> at 700 °C to 1.16 g/cm<sup>3</sup> at 1000 °C with a slight decrease to 1.14 g/cm<sup>3</sup> at 1200 °C which further increases to 1.17 g/cm<sup>3</sup> at 1600 °C. In general, the density increases with the increase in carbonization temperatures up to 1000 °C.

Figure 19 confirms that a higher pressing pressure results in a higher compressive strength for all carbonization temperatures. The compressive strength firstly increases when the carbonization temperatures increase from 700 to 900 °C and decreases thereafter when the temperature increases from 900 to 1600 °C. The increase in the compressive strength is due to the increase in the degree of carbonization as confirmed by the FTIR spectra in Fig. 20. When the temperature increases from 700 to 900 °C, the peaks of the alkyne

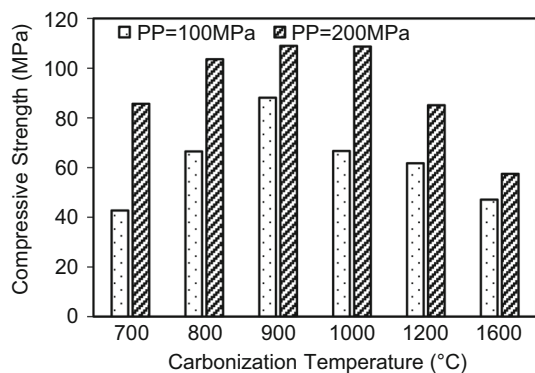


**Figure 19** Compressive strength of CSU samples (MP: PC = 1:2) at six different carbonization temperatures.

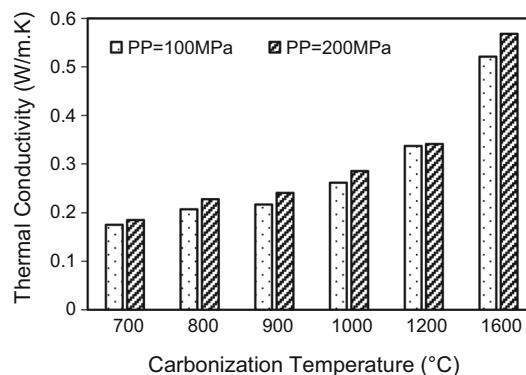


**Figure 22** Thermal conductivity of CSU samples (MP: PC = 1:2) at different carbonized temperatures.

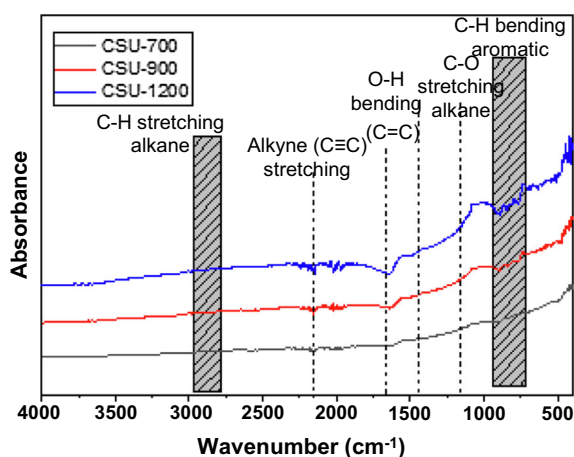


**Figure 20** FTIR analysis of the CSU samples carbonized at three different temperatures. CSU-700, CSU-900 and CSU-1200 represent the CSU samples carbonized at 700 °C, 900 °C, and 1200 °C, respectively.

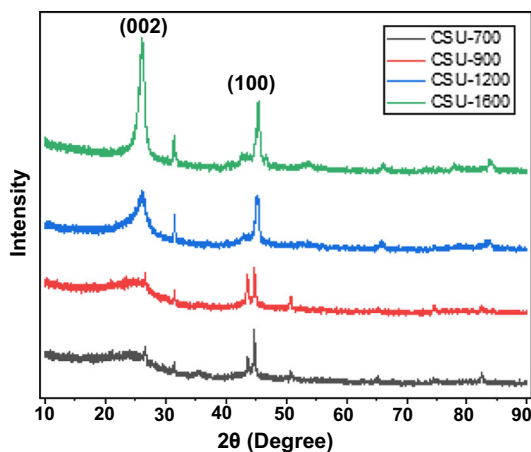


**Figure 21** XRD patterns of CSU carbonized at four different temperatures. CSU-700, CSU-900, CSU-1200 and CSU-1600 represent the CSU samples carbonized at 700 °C, 900 °C, 1200 °C, and 1600 °C, respectively.

(C≡C) stretching at 2100–2250  $\text{cm}^{-1}$  wavenumber [42] increase but the increase is minimal at a higher temperature of 1200 °C. The C≡C bond is the shortest and strongest carbon–carbon bond, and it has the highest bond energy compared to C–C and C=C bonds. Thus, the conversion of carbon bonds into C≡C bond helps to create a strong bond inside the CSU and provide higher compressive strength. Furthermore, a higher temperature than 900 °C increases the degree of graphitization, which makes the CSU sample weaker. This increase in the degree of graphitization reduces the dipole polarization [43] and decreases the compressive strength of CSU. The increase in the degree of graphitization is observed from the XDR pattern of CSU samples in Fig. 21 where the peak (002) at 26 degrees corresponding with the graphitic basal plane increases significantly at temperatures higher than 900 °C (i.e., 1200 and 1600 °C). Furthermore, the collapse of carbon structure at these elevated temperatures reduces the compressive strength. The CSU samples pressed at 200 MPa and carbonized at 900 °C exhibit the highest compressive strength of 109 MPa. Meanwhile, the CSU sample carbonized at 900 °C and pressed at 100 MPa exhibits a relatively high compressive strength of 88.1 MPa. The thermal conductivity increases as the carbonization temperature increases due to the increasing graphitization levels [44] for both 100–200 MPa as depicted in Fig. 22. The thermal conductivity increases from 0.18 to 0.52 W/m K for 100 MPa pressing pressure and it increases from 0.19 to 0.57 W/m K for 200 MPa when the carbonization temperature increases from 700 to 1600 °C. For both of the pressing pressures, thermal conductivity is lower than 0.3 W/m K up to a carbonization

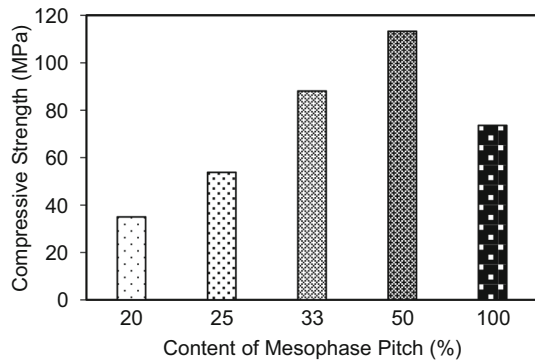


**Figure 23** Effect of MP contents on the compressive strength of CSU at 900 °C.

temperature of 1000 °C. It can be concluded that the carbonization temperature for CSU samples made from MP and PC can be optimized at 900 °C at 100 MPa pressing pressure, to reduce the energy associated with manufacturing the CSU, with a compressive strength of 88.1 MPa and thermal conductivity of 0.22 W/m K (Fig. 23).

### Effect of binder contents

Selecting 100 MPa as the pressing pressure, 900 °C as the carbonization temperature and MP as the binder (described in Sects. “Performances of CTP and MP as binders” to “Effect of carbonization temperatures”), CSU samples are prepared to investigate the effect of binder contents on the compressive strength. For this purpose, CSU samples are prepared at five MP contents of 20%, 25%, 33%, 50%, and 100% with respect to the PC. The compressive strength increases from 35 MPa at 20% MP to 113.3 MPa at 50% MP but decreases to 73.6 MPa at 100% MP content as shown in Fig. 23. The results reveal that the MP content increases the compressive strength of CSU with PC as a solid filler due to increased binding between them. A weaker CSU sample is produced using 100% MP without PC because the PC is stable at a carbonization temperature of 900 °C, due to pyrolysis at 850 °C, which provides structural stability. A 20% MP (i.e., MP: PC = 1:4) can produce CSU samples with a compressive strength of 35 MPa which is greater than the target strength of 30 MPa. CSU at 25% MP (i.e., MP: PC = 1:3) is much stronger (53.8 MPa) than normal concrete with a compressive strength ranging from 11 to 27 MPa [45]. Comparing the average density of CSU of  $\sim 1.00 \text{ g/cm}^3$  with concrete of  $2.8 \text{ g/cm}^3$  [3], the optimized CSU shows

much a higher, over 5 times, strength-to-density ratio ( $53.8 \text{ MPa cm}^3/\text{g}$ ) than that of concrete ( $< 10 \text{ MPa cm}^3/\text{g}$ ). Although 33% MP (i.e., MP: PC = 1:2) and 50% MP (i.e., MP: PC = 1:1) can produce CSU samples with even higher compressive strengths of 88.1–113.3 MPa, respectively, it will increase the material cost as MP is much costlier compared to PC. Hence, a mass ratio of MP to PC = 1:3 is suggested as an optimum mixing ratio for the CSU as a potential building material with higher compressive strength and strength-to-density ratio than concrete. In addition, the thermal conductivity of CSU is lower than 0.3 W/m.K when carbonized at a temperature of 900 °C is lower than that of normal-weight concrete ranging from 0.6 to 3.3 W/m K [46].

### Conclusions

The research was conducted to develop a new building material known as CSU using coal-derived pitches and PC from the PRB coal, WY. Coal tar pitch and coal-derived mesophase pitch are selected along with the PC in a series of experiments to produce CSU samples for laboratory testing and characterization. The effects of pressing pressures, carbonization temperatures, and binder contents on the mechanical and thermal properties of CSU samples are investigated. Compared with normal concrete, optimized CSU samples with a better engineering performance in terms of lower density, higher compressive strength, and lower thermal conductivity are recommended. Based on the experimental results, the following conclusions are drawn:

1. Coal-derived MP has a better binding capacity than CTP to produce CSU samples with higher compressive strengths and lower thermal conductivities.
2. To attain a relatively high compressive strength and low thermal conductivity, a 100 MPa pressing pressure of 100 MPa can be selected to reduce the energy associated with manufacturing CSU.
3. The carbonization temperature of 900 °C produced the CSU samples with the highest compressive strength for the pressing pressure of 100 MPa and this 900 °C can be considered as the optimized carbonization temperature for samples made from MP and PC.

4. A 25% MP content (MP:PC = 1:3) can be considered as an optimized MP content for low-cost CSU fabrication, which has a much lower density, lower thermal conductivity, higher compressive strength, and higher strength-to-density ratio than normal concrete.

## Acknowledgements

The authors would like to acknowledge the funding supports from the Wyoming State Legislator through the School of Energy Resources of the University of Wyoming and the United States Department of Energy (DOE) under the Award No. DE-FE0031996. This manuscript is the result of work sponsored by an agency of the United States Government. Neither the United States Government nor any agency thereof, nor any of their employees, makes any warranty, express or implied, or assumes any legal liability or responsibility for the accuracy, completeness, or usefulness of any information, apparatus, product, or process disclosed, or represents that its use would not infringe privately owned rights. Reference herein to any specific commercial product, process, or service by trade name, trademark, manufacturer, or otherwise does not necessarily constitute or imply its endorsement, recommendation, or favoring by the United States Government or any agency thereof. The views and opinions of the authors expressed herein do not necessarily state or reflect those of the United States Government or any agency thereof. In addition, the content presented in this manuscript is part of the provisional patent application No. 63/355,426.

## Funding

This study was funded by U.S. Department of Energy (grant number DE-FE0031996) and the School of Energy Resources of the University of Wyoming.

## Declarations

**Conflict of interest** Dr. Kam Ng has received research grants from the U.S. Department of Energy and School of Energy Resources. The authors declare that they have no conflict of interest.

## References

- [1] Blander M, Sinha S, Pelton, A, Eriksson, G (1989) Calculations of the Influence of Additives on Coal Combustion Deposits, Argonne National Laboratory. Report No. CONF-890401-8, 340-346
- [2] Jiang T, Liu S, AlMutawa F, Tanner JE, Tan G (2019) Comprehensive reuse of pyrolysis chars from coals for fabrication of highly insulating building materials. *J Clean Prod* 222:424–435
- [3] Wiratmoko A, Halloran JW (2009) Fabricated carbon from minimally processed coke and coal tar pitch as a carbon-sequestering construction material. *J Mater Sci* 44:2097–2100. <https://doi.org/10.1007/s10853-008-3174-0>
- [4] Zhang R, Liu D, Wang Q, Luo Z, Fang M, Cen K (2015) Coal char gasification on a circulating fluidized bed for hydrogen generation: experiments and simulation. *Energ Technol* 3:1059–1067
- [5] Shi M, Xin Y, Chen X, Zou K, Jing W, Sun J, Chen Y, Liu Y (2021) Coal-derived porous activated carbon with ultrahigh specific surface area and excellent electrochemical performance for supercapacitors. *J Alloys Compd* 859:157856-1-10
- [6] Lu Q, Xu Y, Mu S, Li W (2017) The effect of nitrogen and/or boron doping on the electrochemical performance of non-caking coal-derived activated carbons for use as supercapacitor electrodes. *New Carbon Mater* 32:442–450
- [7] Wang L, Sun F, Gao J, Pi X, Pei T, Qie Z, Zhao G, Qin Y (2018) A novel melt infiltration method promoting porosity development of low-rank coal derived activated carbon as supercapacitor electrode materials. *J Taiwan Inst Chem Eng* 91:588–596
- [8] Guo M, Guo J, Jia D, Zhao H, Sun Z, Song X, Li Y (2015) Coal derived porous carbon fibers with tunable internal channels for flexible electrodes and organic matter absorption. *J Mater Chem A Mater* 3:21178–21184
- [9] Yang J, Nakabayashi K, Miyawaki J, Yoon S-H (2016) Preparation of isotropic pitch-based carbon fiber using hyper coal through co-carbonation with ethylene bottom oil. *J Ind Eng Chem* 34:397–404
- [10] Daulbayev C, Kaidar B, Sultanov F, Bakbolat B, Smagulova G, Mansurov Z (2021) The recent progress in pitch derived carbon fibers applications. A review. *S Afr J Chem Eng* 38:9–20
- [11] Chen C, Kennel EB, Stiller AH, Stansberry PG, Zondlo JW (2006) Development of carbon foam using coal-derived precursors. *Carbon* 44(8): 1535-1543
- [12] Zhou P, Chen Q-L (2016) Preparation and characterization of carbon foam derived from coal pitch. *J Anal Appl Pyrolysis* 122:370–376

- [13] Yang N, Gao X, Shen Y, Wang M, Chang L, Lv Y (2022) Effects of coal characteristics on the structure and performance of coal-based carbon foam prepared by self-foaming technique under atmospheric pressure. *J Anal Appl Pyrolysis* 164:105516-1-11
- [14] Leandro APM, Seas MA, Vap K, Tyrrell AS, Jain V, Wahab H, Johnson PA (2021) Evolution of structural and electrical properties in coal-derived graphene oxide nanomaterials during high-temperature annealing. *Diam Relat Mater* 112:108244-1-9
- [15] Li H, He X, Wu T, Jin B, Yang L, Qiu J (2022) Synthesis, modification strategies and applications of coal-based carbon materials. *Fuel Process Technol* 230:107203-1-18
- [16] Zhang C, Xie Y, Zhang C, Lin J (2019) Upgrading coal to multifunctional graphene-based materials by direct laser scribing. *Carbon* 153:585–591
- [17] Wang J, Morishita K, Takarada T (2001) High-temperature interactions between coal char and mixtures of calcium oxide, quartz, and kaolinite. *Energy Fuels* 15:1145–1152
- [18] Xiao J, Zhang L, Yuan J, Yao Z, Tang L, Wang Z, Zhang Z (2018) Co-utilization of spent pot-lining and coal gangue by hydrothermal acid-leaching method to prepare silicon carbide powder. *J Clean Prod* 204:848–860
- [19] Wang J, Qin Q, Hu S, Wu K (2016) A concrete material with waste coal gangue and fly ash used for farmland drainage in high groundwater level areas. *J Clean Prod* 112:631–638
- [20] Liu J, Li B, Zhu J (2018) Investigation on pulverized coal char oxy-combustion behavior at moderate and high temperatures: experiments and a novel developed kinetics modeling. *Ind Eng Chem Res* 57:12264–12277
- [21] Wang P, Du Y, Che D (2019) Experimental study on effects of combustion atmosphere and coal char on NO<sub>2</sub> reduction under oxy-fuel condition. *J Energy Inst* 92:1023–1033
- [22] Glaser B, Lehmann J, Zech W (2002) Ameliorating physical and chemical properties of highly weathered soils in the tropics with charcoal: a review. *Biol Fertil Soils* 35:219–230
- [23] Steiner C, Glaser B, Geraldtes Teixeira W, Lehmann J, Blum WEH, Zech W (2008) Nitrogen retention and plant uptake on a highly weathered central Amazonian Ferralsol amended with compost and charcoal. *J Plant Nutr Soil Sci* 171:893–899
- [24] Halloran JW, Guerra Z (2011) Carbon building materials from coal char: durable materials for solid carbon sequestration to enable hydrogen production by coal pyrolysis. *Mater Challenges Altern Renew Energy*. <https://doi.org/10.1002/9781118019467.ch6>
- [25] Josserand L, Coussy O, de Larrard F (2006) Bleeding of concrete as an ageing consolidation process. *Cem Concr Res* 36:1603–1608
- [26] Winarto S, Candra AI, Siswanto E, Ajiono R (2020) Analysis Causes damage and prevention of concrete. In: *Journal of physics: Conference Series*. IOP publishing, p 042031
- [27] Hossain MTT (2021) Evaluation of mitigation measures, development of an ultra-accelerated test to evaluate asr potential in concrete, and consideration of recycled concrete aggregate in new construction. University of Wyoming, NewYork
- [28] Poursae A (2016) Corrosion measurement and evaluation techniques of steel in concrete structures. In: *Corrosion of steel in concrete structures*, pp 169–191
- [29] Sutan NM, Sinin H (2013) Efflorescence phenomenon on concrete structures. In: *Advanced materials research*. Trans Tech Publ, pp 747–750
- [30] Chandra S (2020) Durability problems in concrete. In: *Polymers in concrete*. CRC Press, pp 27–47
- [31] Bremner TW, Eng P (2001) Environmental aspects of concrete: problems and solutions. In: *All-russian conference on concrete and reinforced concrete*
- [32] ASTM F963–17 (2017) Standard consumer safety specification for toy safety. ASTM Int. <https://doi.org/10.1520/F0963-17>
- [33] RoHS EU (2013) Restriction of the use of certain hazardous substances in electrical and electronic equipment (RoHS). *Off J Eur Communities* 46:19–23
- [34] Jiao Y, Tian W, Chen H, Shi H, Yang B, Li C, Shao Z, Zhu Z, Li S-D (2015) In situ catalyzed Boudouard reaction of coal char for solid oxide-based carbon fuel cells with improved performance. *Appl Energy* 141:200–208
- [35] Odeh AO (2015) Qualitative and quantitative ATR-FTIR analysis and its application to coal char of different ranks. *J Fuel Chem Technol* 43:129–137
- [36] Miura K, Nakagawa H, Hashimoto K (1995) Examination of the oxidative stabilization reaction of the pitch-based carbon fiber through continuous measurement of oxygen chemisorption and gas formation rate. *Carbon* 33:275–282
- [37] Alcañiz-Monge J, Cazorla-Amorós D, Linares-Solano A (2001) Characterisation of coal tar pitches by thermal analysis, infrared spectroscopy and solvent fractionation. *Fuel* 80:41–48
- [38] Guillen MD, Iglesias MJ, Dominguez A, Blanco CG (1992) Semi-quantitative FTIR analysis of a coal tar pitch and its extracts and residues in several organic solvents. *Energy Fuels* 6:518–525
- [39] Liu D, Xiao X, Tian H, Min Y, Zhou Q, Cheng P, Shen J (2013) Sample maturation calculated using Raman spectroscopic parameters for solid organics: methodology and geological applications. *Chin Sci Bull* 58:1285–1298
- [40] Larkin P (2017) *Infrared and Raman spectroscopy: principles and spectral interpretation*, Elsevier

- [41] ISO 22007-2 (2015) Plastics—determination of thermal conductivity and thermal diffusivity—Part 2: transient plane heat source (hot disc) method. INTERNATIONAL STANDARD
- [42] Winter A (2022) Organic chemistry I workbook for dummies, Wiley
- [43] Deng W, Li T, Li H, Liu X, Dang A, Liu Y, Wu H (2022) Controllable graphitization degree of carbon foam bulk toward electromagnetic wave attenuation loss behavior. *J Colloid Interface Sci* 618:129–140
- [44] Zhu W, Meng X, Zhan Y, Li H, Ma J, Liu J, Zhai C, Zhang W, Fang X, Ding T (2018) Carbonization temperature controlled thermal conductivity of graphitic carbon nanoparticles and their polymer composites. *AIP Adv* 8:055332-1-12
- [45] Awodiji CTG, Awodiji OO, Onwuka DO (2016) Re-investigation of the compressive strength of ordinary portland cement concrete and lime concrete. *Int J Geol Agric Environ Sci* 4:12–15
- [46] Asadi I, Shafiqh P, Hassan ZFBA, Mahyuddin NB (2018) Thermal conductivity of concrete: a review. *J Build Eng* 20:81–93

**Publisher's Note** Springer Nature remains neutral with regard to jurisdictional claims in published maps and institutional affiliations.

Springer Nature or its licensor (e.g. a society or other partner) holds exclusive rights to this article under a publishing agreement with the author(s) or other rightsholder(s); author self-archiving of the accepted manuscript version of this article is solely governed by the terms of such publishing agreement and applicable law.